Available online at www.sciencedirect.com

ScienceDirect

journal homepage: http://www.elsevier.com/locate/acme

Original Research Article

Analytical modeling on 3D chip formation of rotary surface in orthogonal turn-milling

Lida Zhu *, *Haonan Li*, *Changfu Liu*

School of Mechanical Engineering and Automation, Northeastern University, China

ARTICLE INFO

Article history:
Received 24 December 2015
Accepted 21 March 2016
Available online

Keywords:
Orthogonal turn-milling
3D chip formation
Cutting parameter
Eccentricity
Modeling

ABSTRACT

Orthogonal turn-milling is a relatively new process technology, the coupling turning and milling processes together and enjoying the advantages of both. However, to the best knowledge of the authors, few studies on the chips of the orthogonal turn-milling have been reported, although the understanding of the chips is important when studying turn-milling mechanism, machining heat and tool wear. In this paper, the analytical models of 3D chips (under both centric and eccentric situations) are proposed based on the orthogonal turn-milling principle and the mathematical expressions of chip thickness and height are obtained considering both side and end cutting edges. Based on the models, numerical analysis is performed to understand the relationships between chip dimensions and cutting parameters. To verify the proposed models and numerical results, the validation experiments are conducted. The comparison shows the consistency between theoretical and experimental results in terms of chip geometries and volumes under different cutting speeds and feed rates. Some findings are presented based on this study, which might provide a theoretical foundation and reference for the orthogonal turn-milling mechanism research.

1. Introduction

As one kind of 'coupling' process, turn-milling is relatively new one in precision manufacture domain. Literally, it is called turn-milling because workpieces and cutting tools are simultaneously given rotary motions. It therefore enjoys advantages of both turning and milling processes as well as excels at machining revolving workpieces, like crankshafts or camshafts. Actually, its strengths are far more than this. Owing to intermittent cuts and simultaneous rotations of tools and workpieces, it keeps low thermal stresses, lowers cutting forces and has good removal rates. What is more interesting is about chips. The chip cross-section profile is a function of engage angle and changes continuously. It consists of two parts. One part is created by side cutting edges and the other part is created by end cutting edges. The chip shape differs depending on the variant or the position of the process (Refs. [1,2,13]). Therefore, it is an important research on 3D chip formation of rotary surface in orthogonal turn-milling.

Some literature have researched on this novel process, but most of them have focused more on kinematics principles, effects of process parameters on surface quality and so on [3–5]. There are also some other studies, which have cared

* *Corresponding author*. Tel.: +86 13889373676.
E-mail address: zld1999@gmail.com (L. Zhu).

http://dx.doi.org/10.1016/j.acme.2016.03.011

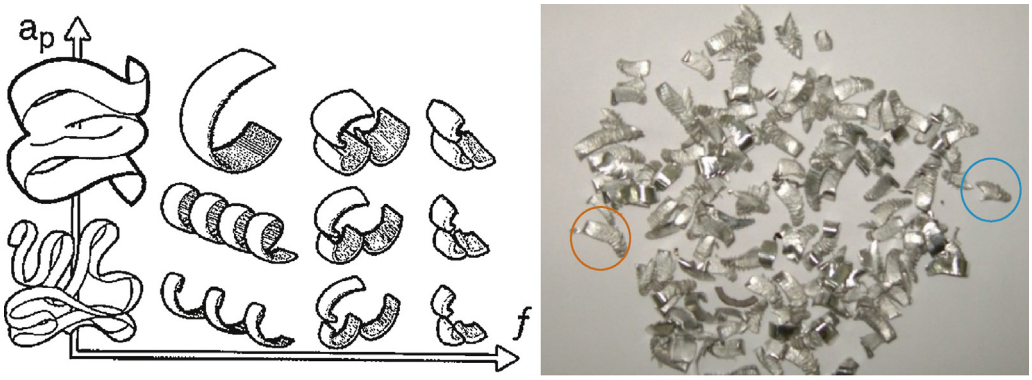

Fig. 1 – Comparison of chip formation by turning and turn-milling. (a) Chip geometry with turning (b) Chip geometry with turn-milling.

more about workpiece surface quality produced by high-speed turn-milling technologies. They have all confirmed that, comparing with the surfaces machined by conventional turning or milling, turn-milling yields a more perfect surface.

However, only a few experts have studies chip formation in orthogonal turn-milling. The first two studies about it are Refs. [6,7] by Schulz. He has proposed some orthogonal turn-milling fundamentals, including kinematics principles, surface finish and geometric accuracy of machined workpiece. He has also concluded that short chips are formed by intermittent cutting process. Later, Jiang has taken a small step forward. In Ref. [8], he has studied that the surface forming mechanism of orthogonal turn-milling and given the mathematical models of orthogonal turn-milling chips, and analyzed the influence of different parameters on the orthogonal turn-milling chip formation by simulation. However, his modeling method of chip formation is complex and only specified for centric condition. Then, after four years, Choudhury and Bajpai in Ref. [10] and Choudhury and Mangrulkar in Ref. [9] have both mentioned that the chips and surface quality of turn-milling are smaller and better than those of turning. Good chip removal has also been achieved due to short chip length. Since several cutting edges are in contact with the workpiece at all times, the effect of the tool during the non-cutting period and the transfer of heat from the machining zone by the chips keep the workpiece temperature relatively low, preventing thermal deformations. Compared with conventional turning, very small chips were produced during the orthogonal turn-milling, especially in the case of mild-steel workpiece. The chip length obtained in turning has been found to be approximately six times more than that obtained in orthogonal turn-milling. Hence, disposal of chips would be very easy in orthogonal turn-milling. Almost at the same time, Jin [11] has concluded that the orthogonal turn-milling chips (when machining high strength steel) belong to sawtooth chip. He has also given the influence of cutting parameter on chip shape, which is regarded as the foundation for chip formation in orthogonal turn-milling. The next attractive study has been conducted by Savas and Ozay in Refs. [12,13]. In the case of tangential turn-milling (a special kind of orthogonal turn-milling, which only involves side cutting edges), they have concluded that, for steel workpiece, it tends to yield smaller chips by turn-milling than those machined by conventional turning. And with a proper selection of rotary speeds, including turning-speed and milling-speed, extraordinary phenomenon during cutting process are observed, for example: the reduction of cutting forces is up to 10%, which guarantee a low coefficient friction, without increasing corresponding metal removal rate. A recent study is developed by Skoric in Ref. [14]. He has first analyzed the suitability of turn-milling process and for the purpose of estimating turn-milling process, a set of functions and methods have been proposed and defined. Chip geometry has been presented in centric position and eccentric position.

According to Ref. [14], the function of the chip geometry is defined by the volume coefficient k_{ch}, i.e.,

$$k_{ch} = \frac{V_{ch}}{V_c} \tag{1}$$

And there are four types of turning chips (shown in Fig. 1 (a)), categorized by their geometry dimensions and shapes. These four types are: (1) unsatisfying chip geometry (k_{ch} = 60–400), whose shapes are long coils of big diameters and long straps; (2) acceptable chip geometry (k_{ch} = 45–60), whose shapes are long coils of small diameters; (3) suitable chip geometry (k_{ch} = 10–45), whose shapes are short coils and spirals; (4) suitable chip geometry (k_{ch} = 5–10), whose shapes are long and short splinter chips. Skoric have summarized that all chips in orthogonal turn-milling belongs to the same chip classification, suitable chip geometry (k_{ch} = 5–10), as shown in Fig. 1(b). And these chips have no influence on the machined workpiece surface quality, avoiding traditional chip's winding.

Besides, from the perspective of methodology, most researchers use finite element method or experimental analysis, like Refs. [15–22]. Exceptions are analytical method, atypical example of which is proposed by Harshad and Liang in Refs. [23,24]. They have confirmed that mathematic modeling approach is accessible when studying uncut chip dimensions in the ball end milling process. It is observed that the analytical models for predicting chip volumes or dimensions match well with the corresponding experimental values.

But regrettably, for orthogonal turn-milling process, the comprehensive chip formation in centric and eccentric positions as well as various cutting parameters' effects on chip shapes and dimensions are significantly lacking. Therefore, this

paper will propose mathematically model 3D chips in orthogonal turn-milling and conduct experimental verification.

This paper is divided into five main sections. Section 1 will give orthogonal turn-milling principle and comparison of chip formation in orthogonal turn-milling with that in turning. Section 2 will present geometrical model of chip formation, in respectively central and eccentric conditions. Section 3 will simulate 3D chip formation and analyze the relations between chip shape and dimension with regard to rotation angle. Section 4 is the experimental verification and analysis part, which suggests that chip geometry volumes matches well with orthogonal turn-milling experimental values. Finally, in Section 5, some conclusions from this study are given.

2. Orthogonal turn-milling principle and parameters

Orthogonal turn-milling is a cutting process superimposing turning and milling together. It can be regarded as a special turning process, in which turning tool is replaced by a milling unit. So, the axes of the cutter and workpiece are orthogonal to each other. This is also why turn-milling operation is able to produce a variety of rotary surface types of workpiece.

Turn-milling involves four basic motions including rotation of cutter, rotation of workpiece, axial and radial feed of cutter, as shown in Fig. 2(a). Rotation of cutter is the main cutting motion. The cutting speed is codetermined by rotational speed of cutting tool and workpiece, wherein rotational speed of cutting tool is a main factor of cutting speed, especially high turn-milling process [25].

A typical cutting period of orthogonal turn-milling is shown in Fig. 2(b). Cutter and workpiece begin to engage at point 1. With the increase of rotation angle of cutter, the cutting depth of side cutting edge is increased and gotten the maximum value at point 2; meanwhile, end cutting edge begins to engage along workpiece axial direction. Owing to axial feed from point 1 to point 2, the depth of cut is large and increasing gradually and the radial cutting depth of side cutting edge decreases slightly. At point 3, the depth of cut is up to the maximum value by end cutting edge and that of side cutting edge are down to the minimum value. Then, the cutting depth of end cutting edge decreased gradually and that of side cutting edge are slightly recovered. At point 4, teeth engage machined surface of workpiece and the cutting depth of side cutting edge decrease rapidly until at point 5, the cut depth of side cutting edge and that of end cutting edge are down to zone simultaneously and a typical period of orthogonal turn-milling is over.

It can be seen that, during each cutting period, several cutting inserts are in contact with the workpiece at the same time, so intermittent cutting and enough quenching time for each cutting edges can be gained. So machining heat transfers more to chips, resulting in low workpiece temperature, little thermal deformation, high surface finish and small tool wear. Meanwhile, good chip removal rate and automatic chip disposal can also be achieved, because the short chips produced in turn-milling, which is given in Fig. 2(c).

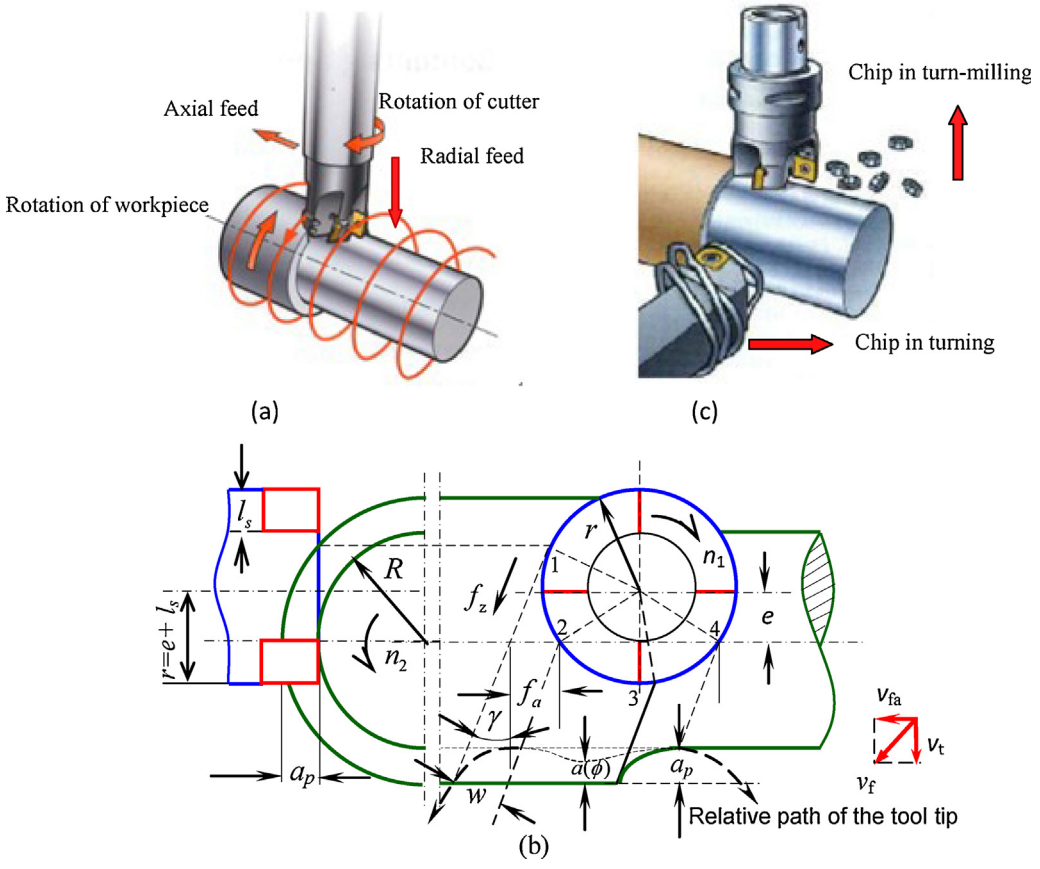

Fig. 2 – The machining kinematic principle in orthogonal turn-milling process.

There are several machining parameters in orthogonal turn-milling, containing rotation speed of cutter, rotation speed of workpiece, cutting speed, axial feed, feed per tooth, and depth of cut and so on. There are also some geometry parameters such as workpiece radius, eccentricity, radius of cutter, teeth of cutter, cutting width, cutting edge geometry and so on.

Some main orthogonal turn-milling parameters are shown as follows:

(1) Cutting velocity

The angular velocity and linear velocity of cutter is considerably higher than those of workpiece in orthogonal turn-milling, so the rotational speed of cutter is considered as a main parameter. The cutting velocity is expressed as follows:

$$v_c = r\cdot\omega_1 = r\cdot 2\pi\cdot n_1. \tag{2}$$

(2) Feed velocity

As illustrated in Fig. 2(c), the feed velocity is composed of axial and tangential feed velocity of cutter relative to workpiece, which can be expressed as

$$|v_f| = \begin{pmatrix} |v_{fa}| \\ |v_t| \end{pmatrix} \tag{3}$$

where the tangential feed velocity (i.e., workpiece velocity) can determined by workpiece speed and circumference of workpiece.

$$v_t = n_2\cdot 2\pi\cdot(\mathrm{R} + a_p) = \omega_2\cdot(\mathrm{R} + a_p) \tag{4}$$

(3) Feed range

The tangential feed range is $f_t = 2\pi\cdot(\mathrm{R} + a_p)$ (5)

The axial feed range is $f_a = v_{fa}/n_2$ (6)

So, the feed range per teeth is expressed as follows

$$f_z = \frac{|v_f|}{zn_1} = \frac{n_2\sqrt{f_a^2 + [2\pi\cdot(\mathrm{R} + a_p)]^2}}{zn_1}. \tag{7}$$

From Eq. (7), it can be seen that the feed range per teeth is related with rotational speed of cutter and workpiece, the axial feed range and number of teeth and so on.

(4) Maximum axial feed and eccentricity

The maximum axial feed is an important parameter in orthogonal turn-milling, which is obtained by adjustment eccentricity. Eccentricity is the least distance between axial cords of cutting tool and workpiece in space, which is related with axial feed and directly effects on cutting efficiency and quality. Here, the relations between eccentricity and axial feed in turn-milling process are analyzed. There are five different eccentricity types shown in Fig. 3.

From the relations between eccentricity and axial feed, it is shown that maximum axial feed is decided by eccentricity, radius and edge geometry of cutter and so on. In Fig. 3(a), end cutting edges and side cutting edges almost start to cutting at the same time. And the former ones complete cutting prior to the latter ones. In Fig. 3(b), end cutting edges begin to cut posterior to and accomplish cutting prior to side cutting edges. In Fig. 3(c), end cutting edges scarcely cut while side cutting edges almost do all the cutting. It is obvious that in this situation there is no compression between end cutting edges and machined surface, so the minimum radial cutting force can be obtained, which is good for high shape accuracy of machined workpiece and result in maximum machining efficiency. In Fig. 3(d) and (e), the cutting zone of side cutting edges are decreasing while that of end cutting edges are increasing. Side cutting edges complete cutting prior to end cutting edges.

The relationship of eccentricity and maximum axial feed is expressed by five points, as seen in Fig. 4. The cylindrical surface is generated in shade zone and thread surface is generated at the right part of the shade zone. The left part of the shade zone is not suitable and should not be chosen in this situation, because it will lead to tool damage.

3. Geometrical models of chip formation

Orthogonal turn-milling is a complex kinematic process, which results in a characteristic cross-section of the chip and its thickness and height changes continuously. The cross-section of the chip is function of the engage angle under certain machining conditions. As shown in Fig. 5, chips in orthogonal turn-milling contain two different parts. One is created by side cutting edge and the other is produced by end cutting edge. Therefore, the engage zone between cutter and workpiece is analyzed in the first stage.

It is noted that, aforementioned cutting zone on milling cutter in orthogonal turn-milling and following discussion are established on some assumptions, which are: (1) Chips peeled from the workpiece are undeformed; (2) Cutting edges are absolutely sharp, no matter how thin cutting layer is, chip can be completely cut down; (3) When the axes of cutter and workpiece are perpendicular to each other, there is no installation error the axes of cutter and workpiece; (4) The side cutting edge and the end cutting edge are perpendicular to each other, and there is no speed error between the workpiece and the cutter.

Modeling of chip geometry mainly includes modeling of chip height and thickness. And the height and thickness are all determined not only by side cutting edge but also by end cutting edge, which should be modeled, separately.

3.1. *Chip height and thickness in centric position*

In centric position, a rotating coordinate is established on tool, whose Y′-axis is in the same direction as helix direction of workpiece (shown in Fig. 6). The relationship between the rotating angle in this created coordinate and that of the original coordinate can be expressed as follows

$$\phi' = \phi + \gamma = \phi + \arccos\left(\frac{f_a}{w}\right) \tag{8}$$

where ϕ' is rotating angle in rotating coordinate; ϕ is rotating angle of cutter in original coordinate.

The center point of milling-tool moves from point O_1 to O_2. When the feed engagement of cutter is termed as f_z, the rotating angle of workpiece can be described as follows:

$$\theta_z = \frac{2\pi n_2}{n_1\cdot z} \tag{9}$$

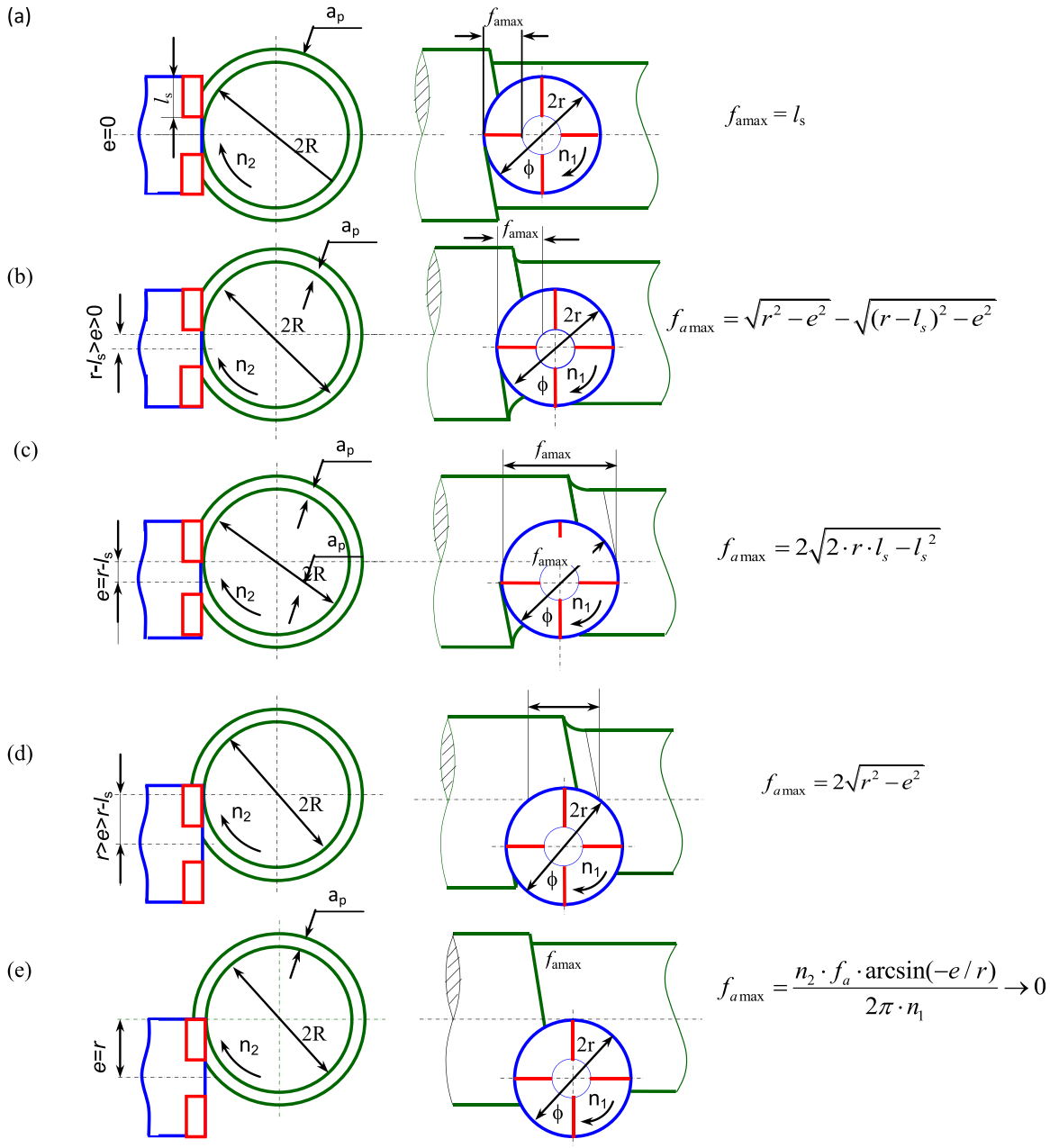

Fig. 3 – The various eccentricities affect feed rate in axial direction.

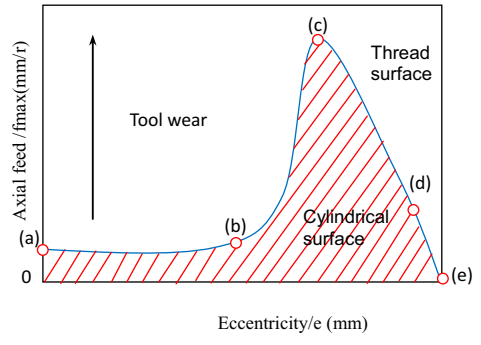

Fig. 4 – The relationship of eccentricity and axial feed.

(1) Chip thickness of side cutting edge

Owing to the direction of chip thickness should always be the same with the direction of cutting speed of tool (shown in Fig. 6), the entry angle ϕ_{pst} and the exit angle ϕ_{pex} of side cutting edge can be written as follows:

$$\phi_{pst} = \arccos\left(\frac{f_z}{2r}\right) \tag{10}$$

$$\phi_{pex} = \pi - \arcsin\left(\frac{r-w}{r}\right) \tag{11}$$

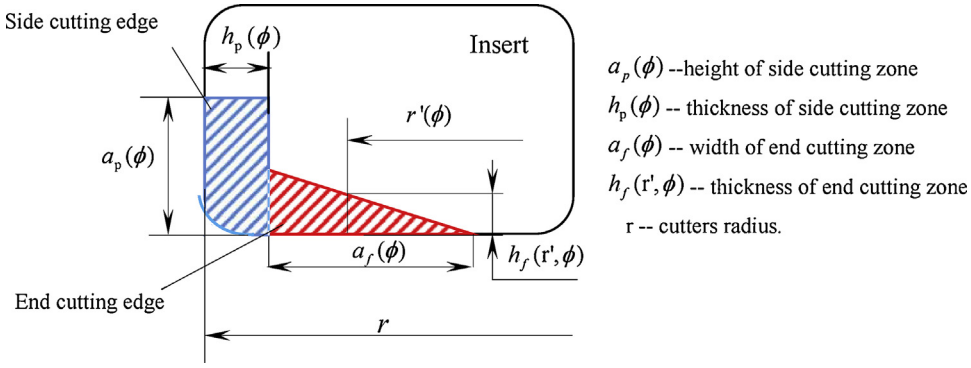

Fig. 5 – Cutting zone on milling cutter in orthogonal turn-milling.

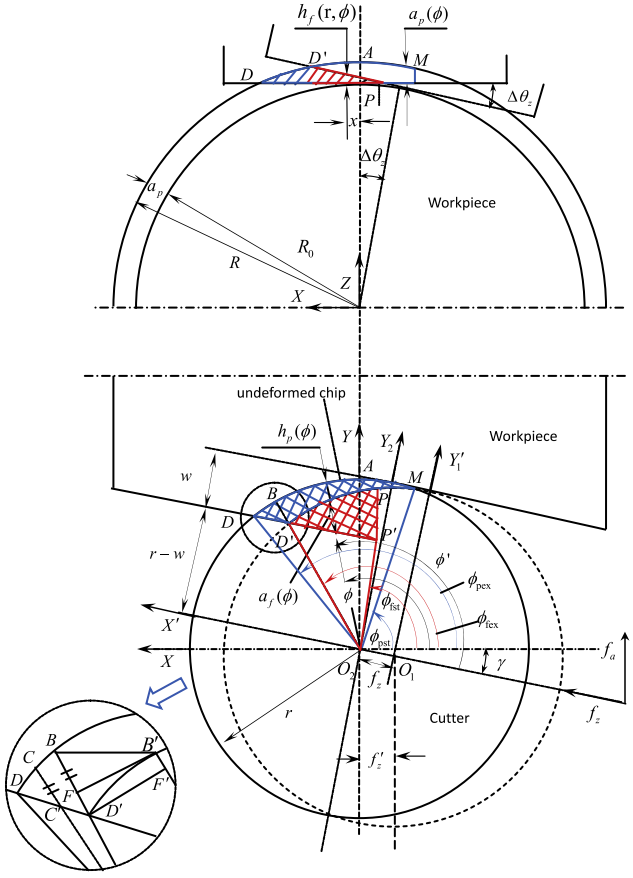

Fig. 6 – Theoretical chip geometry with orthogonal turn-milling (centric position).

The geometrical and mathematical model of chip thickness of side cutting edge is given in Eq. (12):

$$\begin{cases} h_{p1}(\phi) = -f_z\cdot\cos(\phi+\gamma)+r-\sqrt{r^2-(f_z\cdot\sin(\phi+\gamma))^2} & \phi_{pst}\le\phi\le\phi_m \\ h_{p2}(\phi) = r-\dfrac{r-w}{\sin(\phi+\gamma)} & \phi_m\le\phi\le\phi_{pex} \end{cases} \quad (12)$$

where ϕ_m is the rotated angle of tool in $\overline{BD'}$ position, which is $h_{p1}(\phi) = h_{p2}(\phi) = h_{pmax}$ (The maximum of chip thickness).

(2) Chip height of side cutting edge

In order to gain the mathematical model of chip height of side cutting edge, coordinates are founded in milling tool and workpiece, separately, which is shown as Fig. 7.

The angular velocity of tool is

$$\omega_1 = 2\cdot\pi\cdot\phi \quad (13)$$

While the angular velocity of workpiece is

$$\omega_2 = 2\cdot\pi\cdot\theta \quad (14)$$

According to coordinates of tool and workpiece in Fig. 7, the workpiece coordinate can be expressed as:

$$\begin{cases} x = (R+a_p)\cdot\cos\theta \\ y = y_T \\ z = (R+a_p)\cdot\sin\theta \end{cases} \quad (15)$$

While the tool coordinate can be given as

$$\begin{cases} x_T = r\cdot\cos\phi \\ y_T = r\cdot\sin\phi \\ z_T = z-R \end{cases} \quad (16)$$

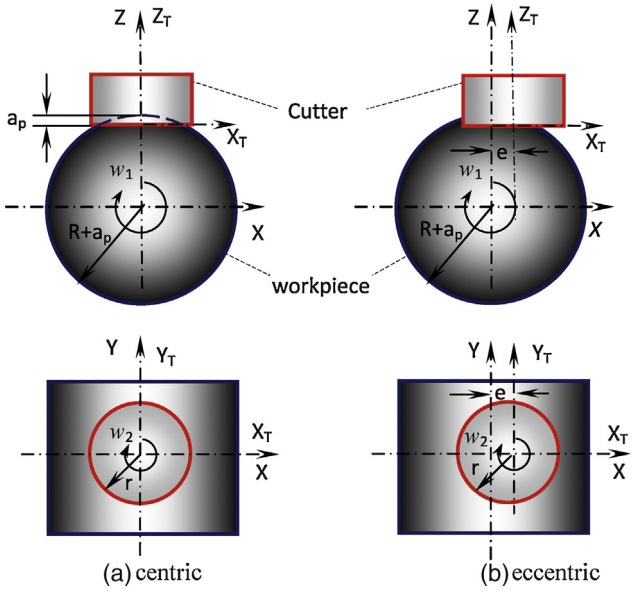

Fig. 7 – Coordinates system of milling cutter and workpiece.

When the eccentricity is zero ($e = 0$), the chip height is

$$a_p(\phi) = -R + \sqrt{(R + a_p)^2 - (r\cdot\cos\phi)^2} \tag{17}$$

When the eccentricity is bigger than zero ($e > 0$), the chip height is

$$a_p(\phi) = -R + \sqrt{(R + a_p)^2 - (r\cdot\cos\phi + e)} \tag{18}$$

(3) Chip width of end cutting edge

The engage zone may be generated by end cutting edge and workpiece in X–Z plane, termed as ''possible engage zone'', which is only projective coincidence zone by end cutting edge and workpiece in the same plane and projective zone of actual engage depending on engage zone in X–Y plane. P point is the cutting entry projective point of the end cutting edge in X–Z plane, D point is the cutting exit projective point of the end cutting edge in X–Z plane, and B point is the cutting exit projective point of the front tooth of cutter of the end cutting edge in X–Z plane. Owing to the chip width of end cutting edge has strong relationship with that of side cutting edge; the analysis should be conducted in the same reference plane.

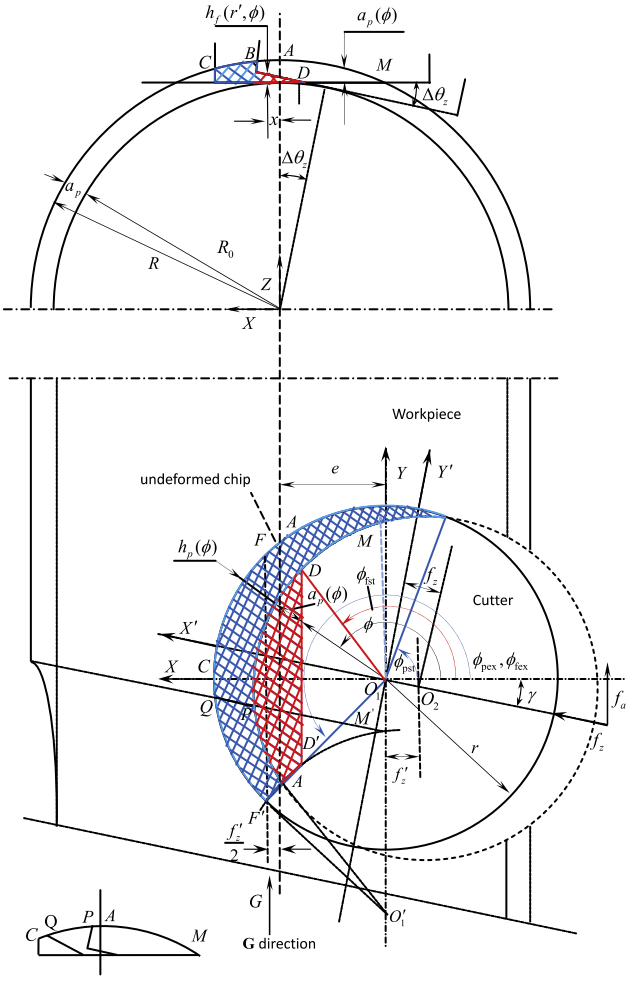

Fig. 8 – Theoretical chip geometry with orthogonal turn-milling (eccentric position).

The entry angle ϕ_{fst} is expressed as follows:

$$\phi_{fst} = \pi - arctg\left(\frac{r-w}{(R-a_{pp})tg(\Delta\theta/2)}\right) - \gamma \tag{19}$$

And the exit angle ϕ_{fex} can be written as follows:

$$\phi_{fex} = \pi - \arcsin\left(\frac{r-w}{r-h_{pmax}}\right) - \gamma \tag{20}$$

The chip width of end cutting edge is expressed as follows:

$$a_f(\phi) = \begin{cases} f_z\cdot\cos(\phi+\gamma) + \sqrt{r^2 - (f_z\cdot\sin(\phi+\gamma))^2} - \dfrac{r-w}{\sin(\pi-\phi+\gamma)} \\ \dfrac{(R-a_p)\cdot\tan(\Delta\theta_z/2)}{\cos(\pi-\phi+\gamma)} - \dfrac{r-w}{\sin(\pi-\phi+\gamma)} \end{cases} \tag{21}$$

(4) Chip thickness of end cutting edge

The chip thickness of end cutting edge is always consistent the direction of feed. When tool rotates once, the thickness can be displayed as follows:

$$h_f(r',\phi) = \begin{cases} ((R-a_p)\cdot tg(\theta_z/2) + r'(\phi)\cdot\cos(\phi))\cdot\tan(\theta_z) & \overline{BD} \\ \sqrt{(R-a_p)^2 - (r'(\phi)\cdot\cos\phi)^2} - (R-a_p) & AB \end{cases} \tag{22}$$

where r' is from the any point of end cutting edge to the center axial of cutter.

3.2. *Chip height and thickness in eccentric position*

(1) Chip thickness of side cutting edge

The calculation model of chip thickness is similar in eccentric case and non-eccentric case. The only difference is the entry angle and exit angle. The direction of chip thickness should always keep consist with the direction of feed per tooth of milling-tool (shown in Fig. 8). As the mentioned above, the entry angle ϕ_{pst} and exit angle ϕ_{pex} can be expressed as follows:

$$\phi_{pst} = \arccos\left(\frac{f_z}{2r}\right) - \gamma \tag{23}$$

$$\phi_{pex} = \pi + \arccos\left(\frac{f_z\cdot\cos\gamma + 2e}{2r}\right) \tag{24}$$

So for orthogonal turn-milling with eccentricity, the chip thickness of side edge is

$$h_p(\phi) = -f_z\cdot\cos(\phi+\gamma) + r - \sqrt{r^2 - (f_z\cdot\sin(\phi+\gamma))^2} \tag{25}$$

(2) Chip width of end cutting edge

The entry angle ϕ_{fst} of end cutting edge is:

$$\phi_{fst} = \pi - \arccos\left(\frac{e}{r}\right) \tag{26}$$

The exit angle ϕ_{fex} of end cutting edge is:

$$\phi_{fex} = \pi + \arccos\left(\frac{f_z\cdot\cos\gamma + e}{2r}\right) \tag{27}$$

The chip width of end cutting edge is

$$a_f(\phi) = r - \frac{2e - 2\cdot(R-a_p)\cdot tg(\theta_z/2)\cdot\cos\gamma}{2\cos(\pi-\phi)} - h_p(\phi) = f_z\cdot\cos(\phi+\gamma) + \sqrt{r^2 - (f_z\cdot\sin(\phi+\gamma))^2} - \frac{(R-a_p)\cdot tg(\theta_z/2)\cdot\cos\gamma - e}{\cos(\phi)} \tag{28}$$

(3) Chip thickness of end cutting edge

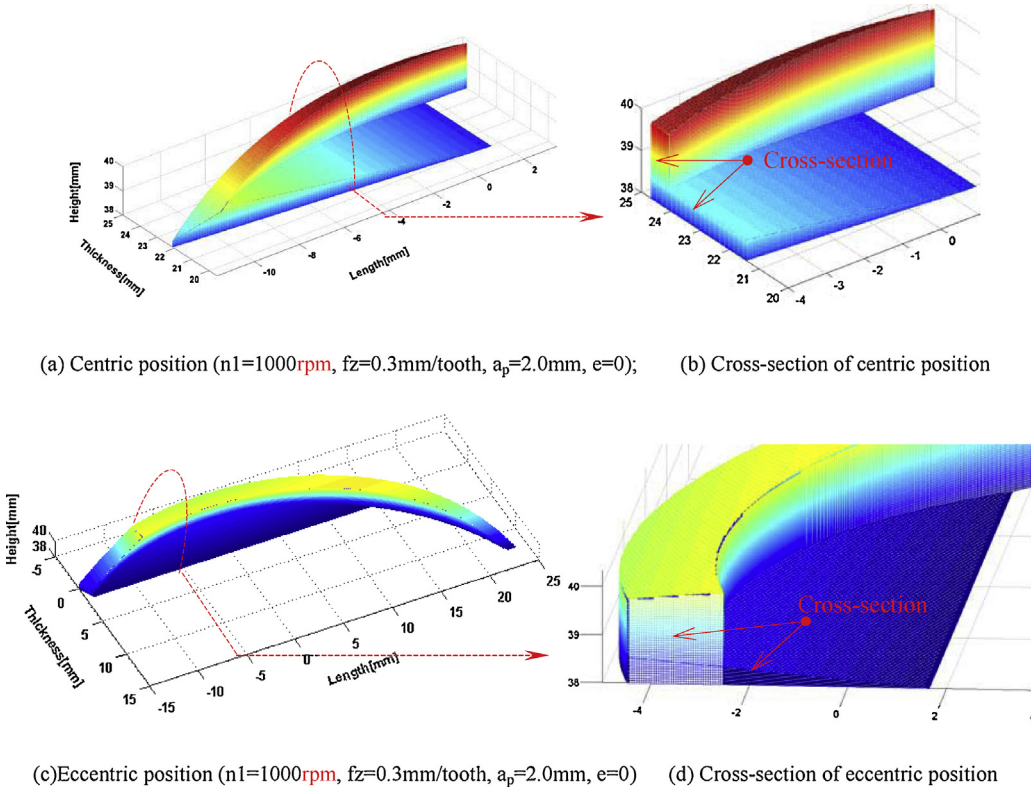

(a) Centric position (n1=1000rpm, fz=0.3mm/tooth, a_p=2.0mm, e=0); (b) Cross-section of centric position

(c)Eccentric position (n1=1000rpm, fz=0.3mm/tooth, a_p=2.0mm, e=0) (d) Cross-section of eccentric position

Fig. 9 – 3D chip formation (undeformed chip).

The distance r' is from the any point of end cutting edge to the center axial of cutter. When tool rotates once, the chip thickness of end cutting edge can be displayed as follows:

$$h_f(r',\phi) = (f_w/2 - e - r'(\phi)\cdot\cos(\phi))tg(\Delta\theta_z) \quad (29)$$

According to all the mathematical models above, the process parameters and eccentricity effects in the aspects of chip thickness and height in both circumferential and end-end cases in turn-milling can be figured out.

4. Simulation analysis of 3D chip formation and relations between chip dimensions and main cutting parameters

After mathematical model of chip is defined, the 3D chip formation of orthogonal turn-milling is simulated by using MATLAB high-level matrix/array language, studying3D chip shape and the effects of the main cutting parameters on the chip dimensions. Taking into account the simultaneous rotation of cutter and workpiece and the superimposition of the feed motion (axial and radial, etc.), the trace of the cutter is discretized into a number of the distinguished revolving positions, depending on the required computational accuracy. The enveloping surface of the cutting edge is considered as the union of the points that belongs to the trace of the cutting edge of the cutting tooth, when it penetrates into workpiece in engage zone. Thereafter, a calculating procedure is utilized to compute the chip cross sections on the development of the side cutting edge and end cutting edge, and in this way to determine the distribution of the undeformed chip formation. A linear interpolation applied between the reference cutting planes to provide a continuous chip. In sequence, the chip geometry is updated for the next tooth penetration by subtracting the intersection area from the cutter reference cutting planes.3D graphical presentations of the undeformed chip geometry are provided by the simulation in centric and eccentric position condition, respectively.

For simulation computation, some initial conditions are given as follows; the workpiece radius R is 40 mm, the length of workpiece L is 50 mm and the cutter radius r is 12.5 mm, and the number of teeth on the cutter z is 4. Considering the different eccentricity between cutting tool and workpiece result in different simulation graphics, cases in centric and eccentric position are shown as follows:

The shapes and cross-sections of chip are visualized in centric and eccentric positions, as shown in Fig. 9. The chip is composed of two parts: a part created by the side cutting edge and a part created by the end cutting edge. It is shown that a complex kinematic process of orthogonal turn-milling has as its consequence a complex operation of the cutting edge, which results in a characteristic cross-section of the chip. The shape and the cross-section of chip differ depending on the variant or position of the process.

In order to study relations between chip dimensions and main orthogonal turn-milling parameters, from Eq. (7), it is shown that feed per tooth plays an important role on orthogonal turn-milling parameters. The effects of feed range

Table 1 – Orthogonal turn-milling parameters.

	n_1 (rpm)	n_2 (rpm)	e (mm)	f_z (mm/z)	a_p (mm)
(a)	4000	10	0	0.5,1.5, 2.5	2
(b)	4000	10	5	0.5,1.5, 2.5	2
(c)	4000	10	2, 5, 8	0.5	2

per teeth and eccentricity on chip dimensions and shapes are studied by simulation analysis based on mathematical model definition of chip formation. The results provide a theoretical foundation and reference for the cutting force and chatter stability of orthogonal turn-milling stability in a further study [25]. The influence regular of chip height and thickness with rotation angle of cutter is obtained in orthogonal turn-milling process. The cutting parameters are as shown in Table 1.

4.1. *Simulation of centric chip dimensions with rotational angle of cutter*

(1) Simulation of chip height and thickness of side cutting edge

When the eccentricity is equal to zero, the chip thickness enlarges with the increase in the feed per teeth in Fig. 10(a). The chip thickness enlarges with the increase in the rotation angle of cutter in the engage zone, which reaches to the maximum when rotation angle increases to 118°, then decreases rapidly. From Fig. 10(b), the chip height is independent of feed per tooth, but the entry cutting angle decreases with increase in feed per tooth and the exit cutting angle is made no difference with increase in feed per tooth.

(2) Simulation of chip height and width in end cutting edge

From Fig. 11(a), chip width enlarges with the increase in the rotation angle of cutter in the engage zone, which reaches to the maximum when rotation angle increases to 75°, then it decreases gradually. The maximum of chip height decreases with the increase in the feed per teeth, but the entry angle is made no difference and the exit angle become small gradually in Fig. 11(b).

4.2. *Simulation of eccentric chip dimensions with rotational angle of cutter*

(1) Simulation of chip thickness of side cutting edge

The relationship between chip thickness of side cutting edge and eccentricity is shown in Fig. 12(a). From the figure above, we can see that entry angle is invariant and exit angle is decreasing with increase of eccentricity. The relationship between chip thickness and feed rate is shown

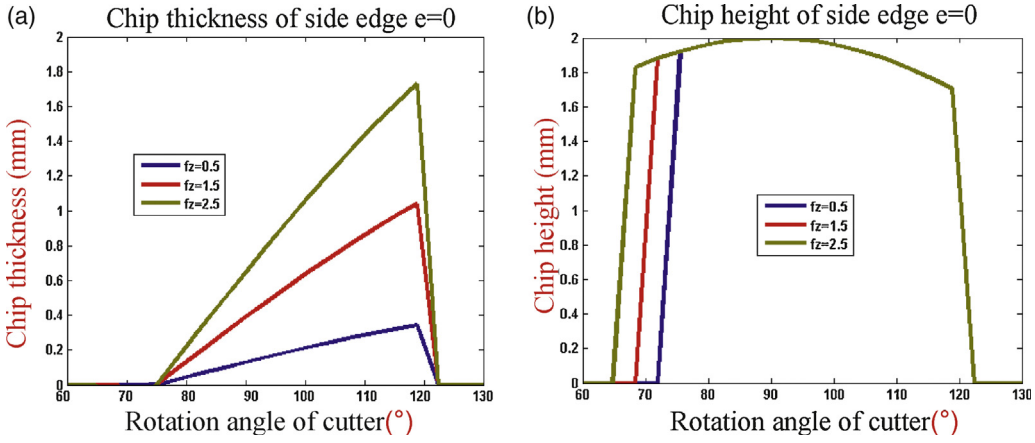

Fig. 10 – Relation between chip height and thickness and rotation angle in side cutting edge.

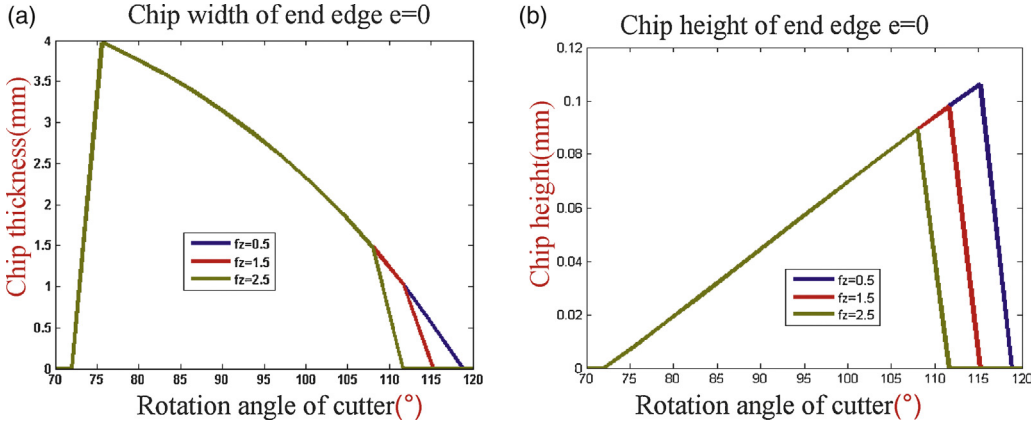

Fig. 11 – Relation between the cutting depth and width and rotation angle in end cutting edge.

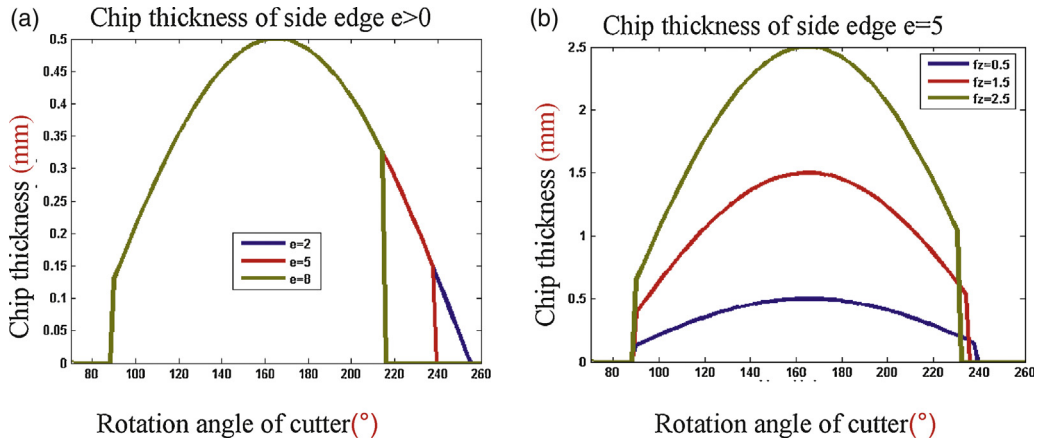

Fig. 12 – The relation between chip thickness and rotation angle.

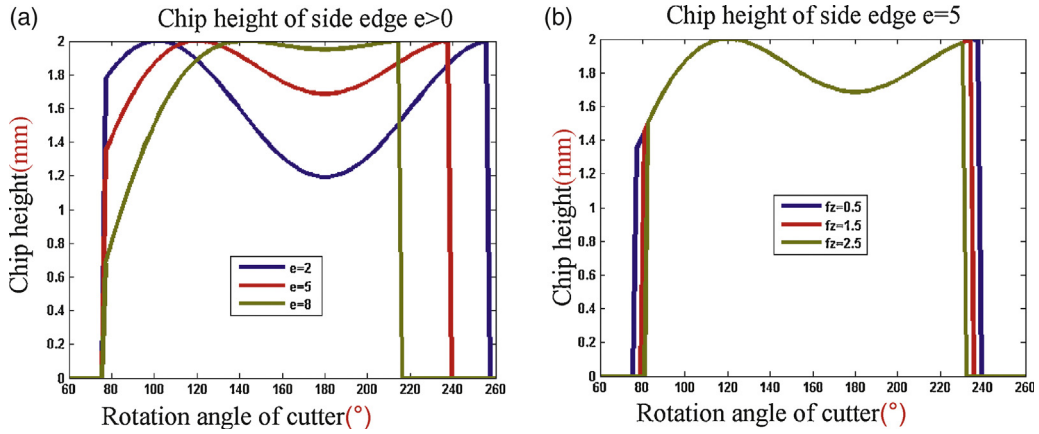

Fig. 13 – The relation between chip thickness and rotation angle.

in Fig. 12(b). From the figure above, we can see that chip thickness increase with increase of feed rate, and entry angle is invariant and exit angle is decreased.

(2) Simulation of chip height of side cutting edge

The relationship between chip height of side cutting edge and eccentricity is shown in Fig. 13(a). From the figure above, we can see that entry angle is invariant and exit angle is decreasing. The relationship between cutting height and feed rate is shown in Fig. 13 (b). From the figure above, we can see that entry angle and exit angle are decreased with increase of feed rate, and chip height is invariant.

(3) Simulation of chip width of end cutting edge

The relationships between chip widths of end cutting edge, feed rate and eccentricity are shown respectively in Fig. 14(a) and (b). From the figures above, we can see that chip width decreases with increase in eccentricity and feed rate but entry angle increases and exit angle is decreasing.

(4) Simulation of chip thickness of end cutting edge

The relationships between chip thickness of end cutting edge and eccentricity are shown respectively in Fig. 13 (a). From the figures above, we can see that chip width increases with increase in eccentricity, but entry angle increases and exit angle is decreasing. The relationships between chip thickness of end cutting edge and feed rate are shown respectively in Fig. 15(a). From the figures above, we can see that chip thickness is invariable, but exit angle is decreasing with increase in federate.

From Figs. 10–15, it is shown that when eccentricity is equal to zero, the entry cutting angle almost start for the end cutting edge and the side cutting edge simultaneously, but the end cutting edge exits from the workpiece before the side cutting edge; In the whole cutting range, the side cutting edge moves to the entry zone, and the end cutting edge will move to the exit zone with the increase of eccentricity. The chip thickness of the side cutting edge and chip width of the end cutting edge increase obviously increases in feed rate.

5. Experiment setup and chip formation analysis

The turn-milling test was conducted in mill-turn center (MORI SEIKI NT3150 DCG), and cutting tool used was 25 mm diameter

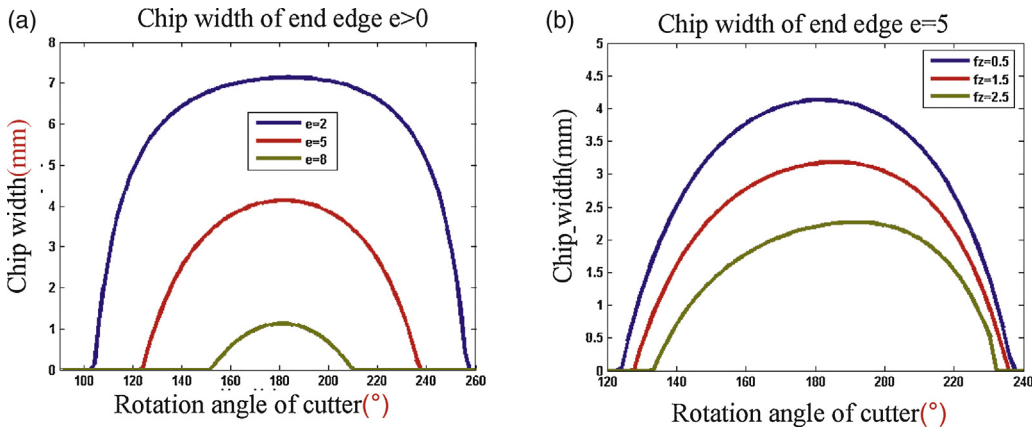

Fig. 14 – The relation between chip width and rotation angle.

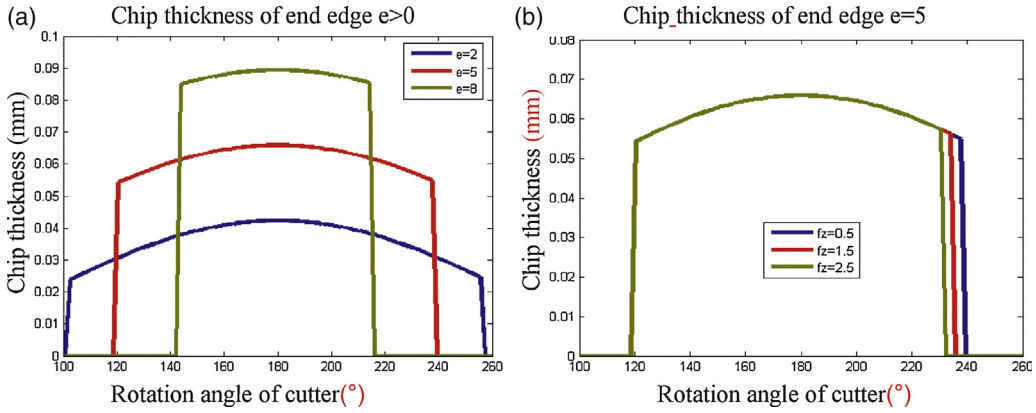

Fig. 15 – The relation between chip height and rotation angle.

end mill (R390-025A25-11H) equipped with four inserts and a tool holder (C5-391 HMD-25-070) made by SANDVIK Inc, as shown in Fig. 16. The insert for CoroMill used is R390-11 T308M-PL, grade1025, which is PVD coated. The insert itself is a rhombic shaped end milling insert with a cutting edge length of 11 mm, a width of 6.8 mm, a 0.8-mm corner radius, and a 90°side cutting edge angle. Since each edge was milled using a fresh cutting edge so that the tool-wear effect on chip formation would be the same and variation due to the wear can be minimized. Cooling method is dry cutting.

The workpiece samples were prepared as 300 mm × ϕ40 mm cylinder and material used in the turn-milling was aluminum alloy 6061-T6. Aluminum alloy combines very General 6061 characteristics and uses: Excellent joining characteristics, good acceptance of applied coatings, relatively high strength, good workability, and high resistance to corrosion; widely available.

The shape and mass of chips are measured respectively by digital microscope (VKEYENCE HX-1000E) and electron weight (Ohaus Explorer) as given in Figs. 17 and 18. The new digital microscope systems provide for clear images, accurate measurement and easy documentation of specimens. The Explorer have multiple weighing mode functions, auto zero tracking and auto tare, which capacities up to 210 g and 0.1 mg readability for maximum accuracy.

5.1. *Comparison of 3D chip geometry between analytical model and experiment result*

The test of chip formation was conducted in different cutting parameters by turn-milling. Comparison of 3D chip geometry between analytical model and experiment result can be obtained, among which: (a) non-eccentric 3D geometry of chips; (b) non-eccentric experimental shape of chips; (c) eccentric 3D geometry of chips; (d) eccentric experimental shape of chips (e = 6 mm) in Fig. 19. Wherein the 3D geometry of chips in Fig. 19(a) and (c) were drawn based on the modeling and simulation analysis, and real 3D shapes of chip in Fig. 19(b) and (d) were obtained in multi-views.

From Fig. 19 above, there are two chip types: non-eccentric and eccentric. Different from turning chips and milling chips, no matter eccentric or non-eccentric, the turn-milling chips is composed by two vertical and linked parts; eccentricity has a bigger influence on the chip shape. Chip thickness is always changed in the revolving direction of milling cutter, namely the variable cutting thickness. For eccentric machining, the part of the chip thickness, which is created by end cutting edge, is small. This part of chip is difficult to cut off if the end cutting edge is not sharp. Owing the change of chip cross-section, the deformation of chips is uneven. It is can be seen that 3D chip geometry model matches well with orthogonal turn-milling experiments.

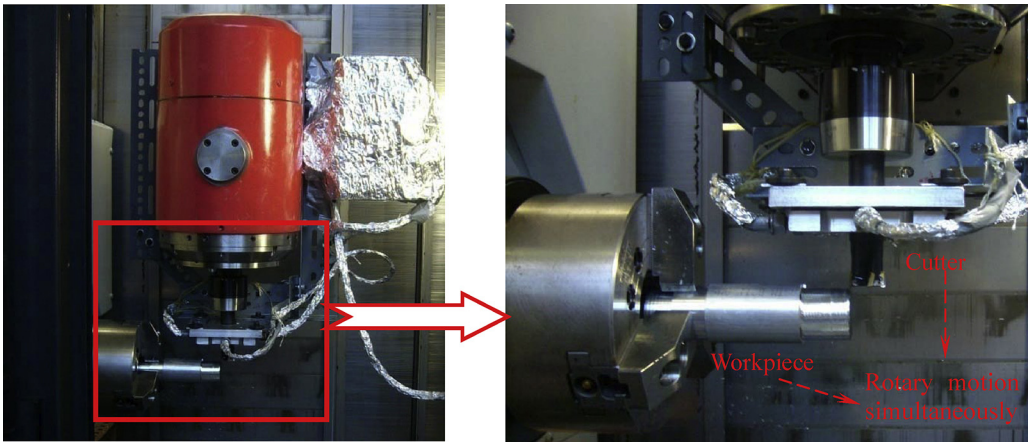

Fig. 16 – The turn-milling test.

Fig. 17 – VKEYENCE HX-1000E digital microscope.

5.2. *Comparison of the predicted volume and measured volume of chips*

The volume of chip is an important parameter to analyze the chip formation. The predicted volume and measured volume of chips are compared by using the volume constancy between the undeformed and the deformed chip dimensions in the same cutting parameters [22]. The volume of chip was calculated by the measured chip's mass based on density of aluminum alloy 6061-T6. In order to improve measure precision, every ten chips are measured together and each measurement is done three times by the Electron Weight, which is given in Fig. 18. The predicted chip volume can be calculated from the model and simulation results. In addition, the comparison of measured and calculated chip's volume was conducted for the no segmented chips.

The predict chip volume and measure chip volume are compared by orthogonal turn-milling in different milling-speed, as shown in Fig. 20. From the above results, it can be noticed that volume of chip decreases with increase in milling-speed in non-eccentric and eccentric position.

The predict chip volume and measure chip volume by orthogonal turn-milling are compared in feed per tooth, as shown in Fig. 21. It can be seen that volume of chip increases with increase in feed per tooth in non-eccentric and eccentric position. And the predicted chip geometry volume matches with experiments well.

In the aspect of material decohesion characterization during turn-milling, the chip compression ratio is an important factor, which effects on chip thickness and chip length. In order to extend the proposed model, the comparison of measured and calculated chip thickness is shown Fig. 22.

It can be seen in Fig. 22 that the predicted chip thickness of side cutting edge matches with experiments. And chip thickness compression ratio is the range (1.05–1.35). In addition, chip thickness increases with the increased feed rate and eccentric chip thickness is larger than in centric condition in the same cutting parameters. So the model of chip formation is feasible and reliable to provide the theoretical foundation and reference for the orthogonal turn-milling mechanism research.

Fig. 18 – Electron weight.

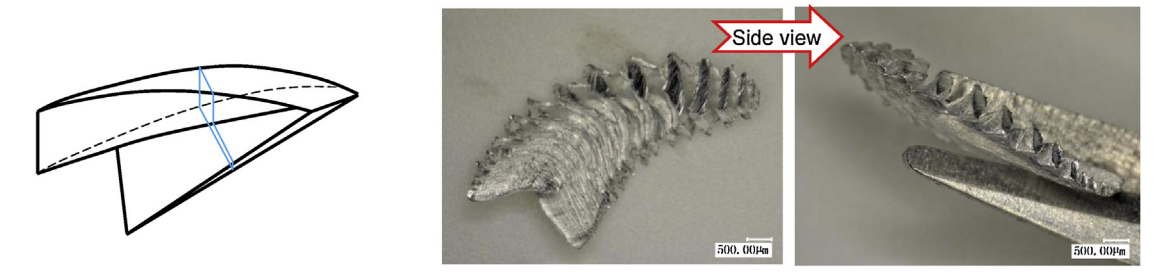

(a) (b)

(Milling spindle speed is 1000rpm; turning spindle speed is 20rpm; depth of cut is 2mm; eccentricity is 0; axial feed velocity is 1.33mm/s.)

(b) (d)

(Milling spindle speed is 1000rpm; turning spindle speed is 20rpm; depth of cut is 2mm; eccentricity is 6mm; axial feed velocity is 1mm/s.)

Fig. 19 – Comparison of 3D theoretical and real chip geometry with orthogonal turn-milling.

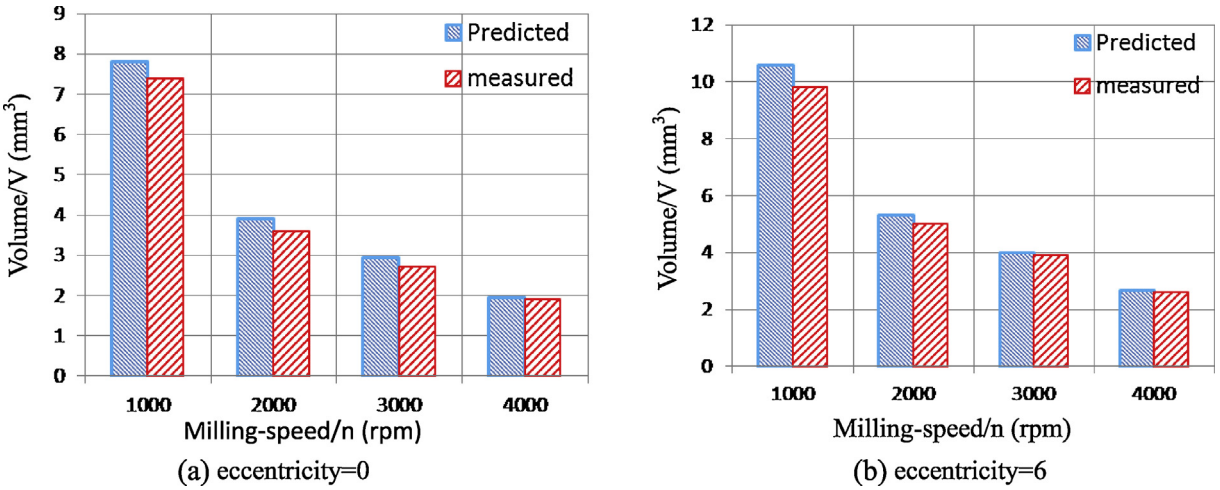

Fig. 20 – Comparison of predicted chip volume and measured orthogonal turn-milling in different milling-speeds (Milling spindle speed is 1000, 2000, 3000, 4000 rpm; turning-spindle speed is 20 rpm; feed per tooth is 0.8 mm/z; depth of cut is 2 mm.).

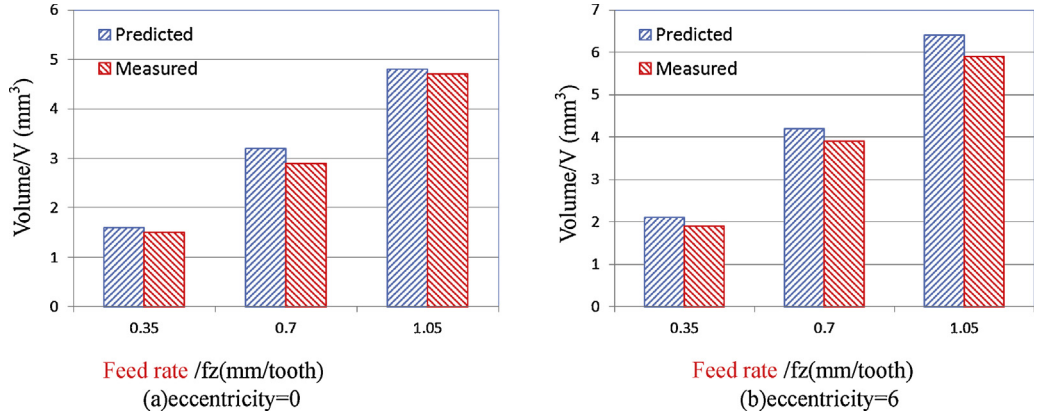

Fig. 21 – Comparison of predicted chip volume and measured orthogonal turn-milling in different feed rate (Milling spindle speed is 1000 rpm; turning spindle speed is 10 rpm; depth of cut is 2 mm; feed per tooth is 0.35, 0.7, 1.05 mm/z.).

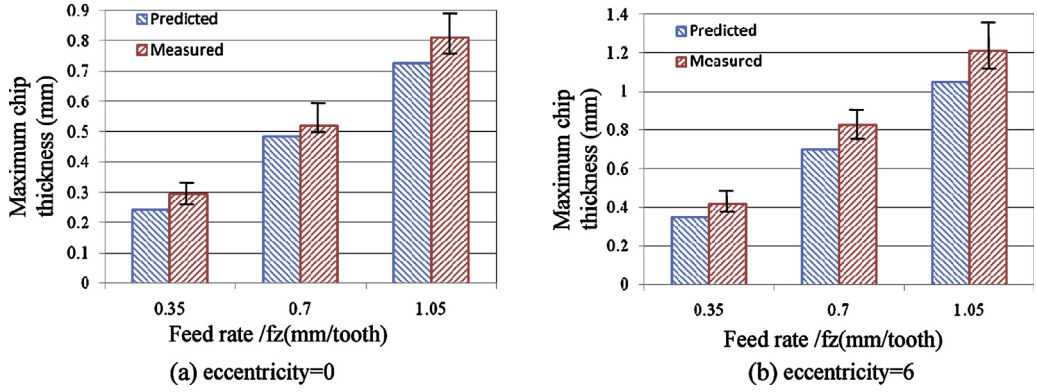

Fig. 22 – Comparison of predicted chip volume and measured orthogonal turn-milling in different feed rate (Milling spindle speed is 4000 rpm; turning spindle speed is 10 rpm; depth of cut is 2 mm; feed per tooth is 0.35, 0.7, 1.05 mm/z.).

6. Conclusions

In this paper, two mathematical models (for centric and eccentric situations) of chips are proposed depending on orthogonal turn-milling principle. We conclude mathematical expressions for chip thickness and height, considering both the side cutting edge and the end cutting edge, respectively. Several new findings may be summarized as followed:

- According to the relation between eccentricity and axial feed, it shows that, when $|e| = r - l_s$, the maximum axial feed is gained, which reach maximum machining efficiency and the workpiece shape accuracy in industrial production. Moreover, the side cutting edge plays a dominant role in eccentricity condition, and the end cutting edge is hardly involved in actual cutting process.
- No matter how much the eccentricity is, chips are consists of two parts. One is created by side edge, the other is generated by end edges. Meanwhile, the cross-section profile of chips is a function of engage angle during processing (in the constant machining condition). Chip thickness is always changing along the direction of the cutter rotation and cutting edge radius has a greater impact on the finishing machining.
- Chip dimensions are affected by various cutting parameters and the influence laws are studied by simulation and experiments. It is shown that when eccentricity is equal to zero, the entry cutting angle almost start for the end cutting edge and the side cutting edge simultaneously, but the end cutting edge exits from the workpiece before the side cutting edge; In the whole cutting range, the side cutting edge moves to the entry zone, and the end cutting edge will move to the exit zone with the increase of eccentricity. The chip thickness of the side cutting edge and chip width of the end cutting edge increase obviously increases in feed rate.
- 3D chip geometry model matches with experiments well. So it is with analytical chip volumes and experiments in different cutting speed and feed rate. Actually, the volume of chip decreases with increase in milling-speed in non-eccentric and eccentric position, but volume of chip decreases with increase in milling-speed in non-eccentric and eccentric position.

Acknowledgements

This work was supported by (National Natural Science Foundation of China) NSFC (51105072) and (51475087), supported by Fundamental Research Funds for the Central Universities (N150304005). Thanks to the University of British Columbia-MAL for helping to complete part of Mill-turn experiment. Thanks to Skoric Ph.D. for helping and providing technology of orthogonal turn-milling in *Croatia*.

REFERENCES

[1] A. Schubert, A. Nestler, R. Funke, Influence of cutting edge geometry and cutting parameters on surface finish in turn milling, Materialwissenschaft und Werkstofftechni 1 (9) (2010) 795–801.
[2] E. Budak, A. Çomak, E. Öztürk, Stability and high performance machining conditions in simultaneous milling, CIRP Annals – Manufacturing Technology 62 (1) (2013) 403–406.
[3] J. Kopac, M. Pogacink, Theory and practice of achieving quality surface in turn-milling, International Journal of Machine Tools Manufacture 37 (5) (1997) 709–715.
[4] S. Ekinovic, E. Begovic, A. Silajdzija, Comparison of machined surface quality obtained by high-speed machining and conventional turning, Machining Science and Technology 1 (4) (2007) 531–551.
[5] M. Pogacink, J. Kopac, Dynamic stabilization of the turn-milling process by parameter optimization, Proceedings of the Institution of Mechanical Engineers Part B – Journal of Engineering Manufacture 214 (2) (2000) 127–135.
[6] H. Schulz, High speed turn-milling – a new precision manufacturing technology for the machining of rotationally symmetrical workpieces, Annals of the CIRP 39 (1) (1990) 107–109.
[7] H. Schulz, T. Kneisel, Turn-milling of hardened steel – an alternative to turning, Annals of the CIRP 3 (1) (1994) 93–96.
[8] Z.H. Jiang, C.D. Jia, Research on the forming mechanism of surface machined by orthogonal turn-milling, Chinese Journal of Mechanical Engineering 4 (9) (2004) 121–123.
[9] S.K. Choudhury, K.S. Mangrulkar, Investigation in orthogonal turn-milling for the machining of rotationally symmetrical workpieces, Journal of Materials Processing Technology 99 (2) (2000) 120–128.
[10] S.K. Choudhury, J.B. Bajpai, Investigation in orthogonal turn-milling towards better surface finish, Journal of Materials Processing Technology 170 (7) (2005) 487–493.
[11] C.Z. Jin, C.D. Jia, Research on mechanism of chip formation in orthogonal turn-milling high strength steel, Journal of Harbin Institute of Technology 5 (9) (2006) 1610–1612.
[12] V. Savas, C. Ozay, The optimization of the surface roughness in the process of tangential turn-milling using genetic algorithm, International Journal of Advanced Manufacturing Technology 37 (4) (2008) 335–340.
[13] V. Savas, C. Ozay, Analysis of the surface roughness of tangential turn-milling for machining with end cutting tool, Journal of Materials Processing Technology 186 (6) (2007) 279–283.
[14] S. Skoric, T. Udiljak, D. Ciglar, Study of the suitability of the machining of rotating surfaces, Transactions of Fame 32 (3) (2008) 69–83.
[15] K.D. Bouzakis, O. Friderikos, I. Tsiafis, FEM-supported simulation of chip formation and flow in gear hobbing of spur and helical gears, Journal of Manufacturing Science and Technology 1 (2008) 18–26.
[16] M. Sima, T. Ozel, Modeling material constitutive models for serrated chip formation simulations and experimental validation in machining of titanium alloy Ti-6Al-4V, International Journal of Machine Tools & Manufacture 50 (2010) 943–960.
[17] J. Lorentzona, N. Jarvstrat, B.L. Josefson, Modelling chip formation of alloy 718, Journal of Materials Processing Technology 209 (2009) 4645–4653.
[18] J. Sun, Y.B. Guo, A new multi-view approach to characterize 3D chip morphology and properties in end milling titanium Ti-6Al-4V, International Journal of Machine Tools & Manufacture 48 (2) (2008) 1486–1494.
[19] J.C. Aurich, H. Bil, 3D finite element modelling of segmented chip formation, Annals of the CIRP 55 (1) (2006) 33–36.
[20] S. Sun, M. Brandt, M.S. Dargusch, Characteristics of cutting forces and chip formation in machining of titanium alloys, International Journal of Machine Tools & Manufacture 49 (5) (2009) 561–568.
[21] G. Sutter, G. List, Very high speed cutting of Ti-6Al-4V titanium alloy – change in morphology and mechanism of chip formation, International Journal of Machine Tools & Manufacture 66 (6) (2013) 37–43.
[22] H. Jiang, R. Shivpuri, Prediction of chip morphology and segmentation during the machining of titanium alloys, Journal of Materials Processing Technology 50 (6) (2004) 124–133.
[23] A.S. Harshad, S. Joshi, Analytical modeling of chip geometry and cutting forces in helical ball end milling of superalloy Inconel 718, International Journal of Machine Tools & Manufacture 3 (3) (2010) 204–217.
[24] X.G. Liang, Z.Q. Yao, An accuracy algorithm for chip thickness modeling in 5-axis ball-end finish milling, Computer-Aided Design 3 (5) (2011) 971–978.
[25] L.D. Zhu, H.N. Li, W.S. Wang, Research on rotary surface topography by orthogonal turn-milling, International Journal of Advanced Manufacturing Technology 9 (5) (2013) 2279–2292.